HEP'97 #535
Submitted to Pa 7, 8
Pl 15

DELPHI 97-114 CONF 96
20 July, 1997

Measurement of the $|V_{cs}|$ using W-decays at LEP-2

Preliminary

DELPHI Collaboration

M.Battaglia[1], B.Eržen[2], B.Golob[2], D.Liko[3], T.Podobnik[3,4,5], S.Stanič[2], A.Tomaradze[6]

Abstract

Decays of $W^{\pm}$-bosons, produced at LEP-2, can be exploited to measure the $|V_{cs}|$ element of the Cabibbo-Kobayashi-Maskawa matrix. The value can be extracted either from the measured hadronic branching ratio of $W^{\pm}$-decays or by tagging the flavour of hadronic jets, produced in $W^{\pm}$-decays. Applying the two methods on the data, collected during the first year of the LEP high-energy run, DELPHI obtains $|V_{cs}| = 0.89\ ^{+0.14}_{-0.13}\ (\mathrm{stat})\ \pm 0.05\ (\mathrm{syst})$.

Paper submitted to the HEP'97 Conference
Jerusalem, August 19-26

[1]Helsinki Institute of Physics, FTN-00014 Helsinki, Finland
[2]J. Stefan Institute, Jamova 39, SI-1000 Ljubljana, Slovenia
[3]CERN, CH1211 Geneva 23, Switzerland
[4]Department of Physics, University of Oxford, Keble Road,Oxford OX11 QQX, UK
[5]Department of Physics, University of Ljubljana, Jadranska 19, SI-1000 Ljubljana, Slovenia
[6]Physics Department, Univ. Instelling Antwepen, Universiteitsplein 1, B-2610 Wilrijk, Belgium

1 Introduction

In the Standard Model with $SU(2) \times U(1)$ as the gauge group of the electroweak interaction, the quark mass eigenstates are not the same as the weak eigenstates. For the six quarks, the two bases are related by the unitary 3×3 Cabibbo-Kobayashi-Maskawa (CKM) matrix [1, 2, 3]. Apart from the matrix elements describing the decays of the heavy t-quark, the value of the element relating the quarks of the second generation is known with the poorest precision. The absolute error on the $|V_{cs}|$, determined in semileptonic decays of D mesons [3], is 18% and is dominated by the poorly known hadronic form-factors.

Hadronic decays of charged weak bosons $W^{\pm}$, produced in the e^+e^- interactions at the upgraded LEP-2 collider, offer an alternative measurement. Namely, in the decays $W^{\pm} \to q_1\overline{q}_2$, the coupling of the $W^{\pm}$ to the quarks q_1 and $\overline{q}_2$ is proportional to the appropriate CKM matrix element $V_{q_1 q_2}$. Therefore, from the measured rate of the $W^+ \to c\overline{s}$[7] decays one can extract the value of the $|V_{cs}|$.

The $|V_{cs}|$-value reflects in the ratio of the overall hadronic $W^{\pm}$-decays to the leptonic decays. By measuring the hadronic branching ratio of the $W^{\pm}$'s and by setting all other parameters of the Standard Model to the presently known values, one can therefore determine the $|V_{cs}|$.

An additional piece of information can be obtained by tagging the flavour of jets produced in hadronic $W^{\pm}$-decays. The flavour of primary quarks, arising from a $W^{\pm}$-decay, is heavily veiled in the process of hadronization. Nevertheless, some of the properties of the resulting hadronic jets can still reveal the information about the jet origins. Tagging the flavour of jets in the DELPHI spectrometer is based upon the measured impact parameters and particle identification.

The results of the two methods are independent and can therefore be combined in order to improve the overall precision of the measurement.

2 The DELPHI detector

A detailed description of the DELPHI apparatus and its performance can be found elsewhere [4, 5]. In what follows, we briefly review the most important properties of the detector relevant to the described measurements.

The detector consists of a cylindrical section, covering the barrel region, and two end-caps. A large superconducting solenoid provides a magnetic field of 1.2 T inside the central tracking volume. The tracking part of the detector consists of the Vertex Detector (VD), Inner Detector (ID), Time projection Chamber (TPC), Outer Detector (OD) in the barrel region, and forward chambers. The VD was composed of three layers of silicon microstrip modules covering the polar angle intervals between 25° and 155° (innermost layer) and 44° and 136° (outermost layer). In 1996 the cylindrical part of the VD was lengthened and extended with additional silicon detectors, covering the end-cap region. The ID and the TPC cover the polar angles between 20° and 160° while the OD essentially improves the momentum resolution for fast particles with $42^\circ \leq \theta \leq 138^\circ$. The combined performance of the tracking detectors results in a relative momentum resolution better than 1% for charged particles with the momenta around 1 GeV/c in hadronic jets, emitted in a direction perpendicular to the beam axis. For such particles the

[7] Throughout the paper references to a specific charge state are meant to imply the charge conjugate state as well, unless explicitly stated otherwise.

impact parameter with respect to the interaction point is determined with an accuracy of around 70 μm.

The barrel and the forward electromagnetic calorimeters are used to measure the deposited electromagnetic energy of particles with $43^\circ \leq \theta \leq 137^\circ$ and $10^\circ \leq \theta \leq 36.5^\circ$, $143.5^\circ \leq \theta \leq 170^\circ$, respectively. The hadron calorimeter measures the energy of hadrons with the polar angle larger than 10°.

Electron candidates are identified by the characteristic energy deposition in the electromagnetic calorimeters. Efficiency for the detection of high-momentum electrons, determined by the simulation and by the measurement of Bhabha events, is (77$\pm$2)%. Muons are recognized by the associated hits in the muon chambers, surrounding the hadron calorimeter, and by the energy deposition in the hadronic calorimeter, compatible with the deposition of a minimum ionizing particle. Efficiency for the identification, obtained by the simulation and from the measured $Z^0 \to \mu^+\mu^-$ decays, is estimated to be (92$\pm$1)%.

Identification of charged hadrons, on the other hand, relies on the specific ionization energy loss per unit length (dE/dx) in the TPC, and on the information from the system of Ring Imaging Cherenkov (RICH) counters. The latter consists of two independent detectors, the Barrel and the Forward RICH, covering together over 90% of the full solid angle. Each of the RICH detectors contains two radiators of different refractive indices, allowing in this way for particle identification in the momentum range between 0.7 and 25 GeV/c. In the present analysis the HADSIGN tagging routine is used[5]. The algorithm provides charged kaon identification with efficiencies between 80% and 45%, and corresponding purities between 60% and 85%, depending on the particle momentum and quality of the track reconstruction.

Simulated W^+W^--events, used in the analysis, were generated with the PYTHIA 5.7 generator [6]. The fragmentation model, incorporated in the simulation, is tuned to the DELPHI data measured at LEP-1 [7].

3 Determination of the $|V_{cs}|$ from the hadronic branching ratio of the W

The $|V_{cs}|$-dependence of the $e^+e^- \to W^+W^-$ cross-section can be parametrized as [8]

$$\sigma(e^+e^- \to W^+W^-) = \sigma_0(e^+e^- \to W^+W^-)\frac{\Gamma_W^2(k)}{\Gamma_W^2(k=1)}f(k)\,, \qquad (1)$$

where k is the ratio between the $|V_{cs}|^2$ and the nominal $|V_{cs}|_0^2 = 0.9493 \pm 0.0008$, determined from the CKM unitarity constraint [3]. The cross section $\sigma_0(e^+e^- \to W^+W^-)$ is calculated with the nominal $|V_{cs}|_0$ and includes corrections due to the initial state radiation, Coulomb corrections and effects of the off-shell W^+W^--production. The total width of the $W^\pm$ is

$$\Gamma_W(k) = k\Gamma_{c\overline{s}} + \sum_{i \neq c\overline{s}} \Gamma_i\,,$$

where i runs over all $W^\pm$-decay modes apart from the $c\overline{s}$ channel. An additional correction factor $f(k)$ (see Fig. 1.a) comes from the $|V_{cs}|$-dependent total widths in the $W^\pm$-propagators. Consequently, the value of the $|V_{cs}|$ reflects in rates also for the decays others than $W^+ \to c\overline{s}$. It turns out that the ratios of the fully hadronic to the mixed and to the fully-leptonic decays of W-pairs are sensitive to such changes while the total number of produced W-pairs is, to a very good approximation, insensitive to the value of the $|V_{cs}|$ (see Figure 1.b).

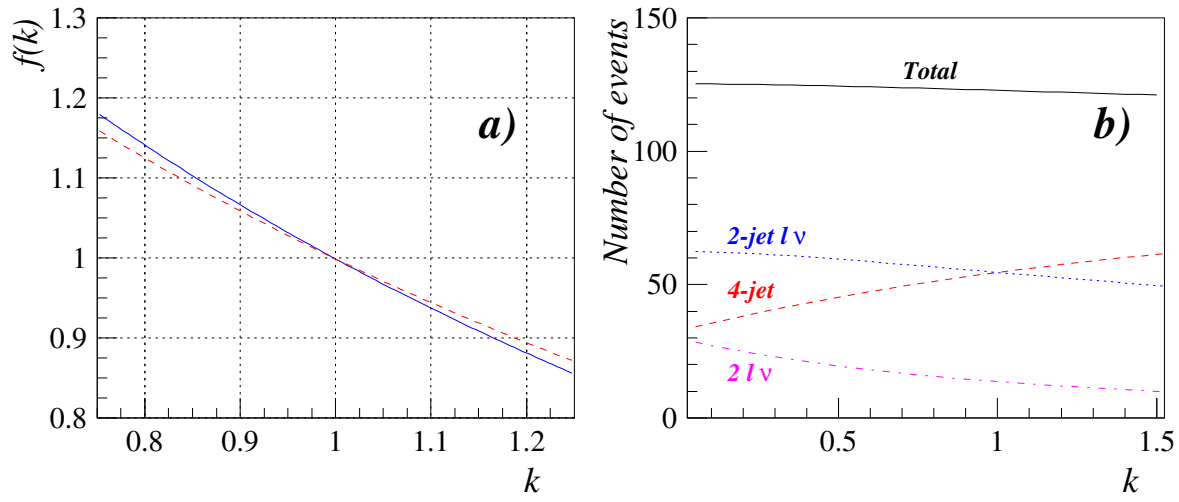

Figure 1: a) Correction factor to the $e^+e^- \to W^+W^-$ cross section, coming from the $|V_{cs}|$-dependent widths Γ_W in the $W^{\pm}$-propagators. The full line shows the correction for the 172 GeV centre-of-mass energy and the dashed line the correction for 161 GeV. b)Number of fully hadronic, mixed and fully leptonic decays of W-pairs with respect to the ratio $|V_{cs}|^2/|V_{cs}|^2_0$. The numbers correspond to an integrated luminosity of approximately 10 pb^{-1} at 172 GeV centre-of-mass energy and were evaluated in the leading-order approximation.

When extracting the $|V_{cs}|$ one can therefore neglect the value of the total cross-section and use only the measured hadronic branching ratio of the W. The analysed data were collected with the DELPHI spectrometer at the e^+e^- centre-of-mass (CMS) energies of 161 GeV and 172 GeV and correspond to the integrated luminosities of 9.93 pb^{-1} and 9.98 pb^{-1}, respectively. Combining the results from the two samples, DELPHI obtains [9]:

$$BR(W \to \text{hadrons}) = 0.660 \, ^{+0.036}_{-0.037} \, (\text{stat}) \, \pm 0.009 \, (\text{syst}) \, .$$

Assuming all other parameters of the Standard Model to be fixed at the presently measured values [3], the measured branching ratio can be converted into

$$|V_{cs}| = 0.90 \, \pm 0.17 \, (\text{stat}) \, \pm 0.04 \, (\text{syst}) \, .$$

The systematic error on the $|V_{cs}|$ includes also a contribution due to uncertainties on the other parameters of the Standard Model (e.g. uncertainties on α_S and $|V_{cd}|$; see Table 1).

4 Tagging the flavour of hadronic jets

An additional information about the $|V_{cs}|$ value can be obtained by tagging the flavour of hadronic jets, arising from fragmentation of the primary quarks from the $W^{\pm}$-decays. Before the flavour tagging, W^+W^--enhanced samples were selected as described in the following paragraphs.

In an event, charged particles were selected within a polar angle between 10° and 170° and with a momentum between 0.4 GeV/c and the beam momentum. In addition, the length of the reconstructed tracks had to be larger than 15 cm, their impact parameters, both longitudinal and

transverse with respect to the beam axis, should not exceed 4 cm, while the maximum allowed uncertainty on the momentum measurement was 100%. Neutral particles, on the other hand, were accepted if they deposited more than 0.5 GeV energy in the electromagnetic or hadronic calorimeters. For each event all selected particles were clustered into jets using the LUCLUS algorithm [6]. To accept a particle in a jet, a maximal distance [6] $d_{ij} = 6.5\ \mathrm{GeV}^2/\mathrm{c}^2$ between the particle and the jet was allowed.

Events were then arranged in three classes: fully hadronic decays where both W^+ and W^- decayed into quarks, mixed decays where one of the two gauge bosons decayed into an electron or a muon and an appropriate neutrino, and mixed decays with a tau lepton and a tau neutrino. For the $W^+W^- \to q_1\overline{q}_2q_3\overline{q}_4$ candidates, the number of reconstructed hadronic jets was required to be at least three. All particles were then forced into a four jet configuration and, in order to improve the momentum and energy resolution, a kinematically constrained fit was performed [12], imposing the momentum conservation and the nominal $W^{\pm}$-mass to di-jet combinations. In an event, the jet pairing which minimized the χ^2 of the fit was chosen. For the $W^+W^- \to q_1\overline{q}_2e^-(\mu^-)\overline{\nu}_{e(\mu)}$ candidates, an isolated track of a highly energetic particle, i.e. a lepton candidate, was required. In particular, in an event the particle with the smallest value for the ratio $(\sum_j p_j)/p_i$ was chosen, where p_i is the momentum of the candidate while the sum runs over momenta of all particles in a 20° cone around the candidate's direction. The remaining tracks were then forced into a two-jet topology. In the case of candidates for the tau lepton mixed decays, on the other hand, the events were forced into configurations with three hadronic jets. In addition, at least one tau-jet candidate was required, identified as a low energy lepton or a low multiplicity narrow jet, isolated from the rest of the event. Requirements, concerning the reconstructed energy and the particle multiplicity of the events, were very mild so that they did not reject any W-pair decays but they did diminish some of the background, e.g. a great deal of $\gamma\gamma$ events. At this stage a single event could also enter more than one of the three classes.

After the preselection, several kinematical properties of the events were combined in order to separate the W-pair signal from the remaining background. For the fully hadronic channel, the number of originally reconstructed jets, the energy of these jets, the probability for the kinematically constrained fit, the angle between the fastest jets from each of the two chosen di-jets, and the effective CMS energy were used. The latter was estimated from the photon radiated off the initial e^+e^- state. For this purpose either the energy of an isolated highly energetic photon was used if such a photon was reconstructed in the detector, or the photon direction was assumed to be parallel to the beam axis and the photon momentum was calculated under the assumption of a two-jet topology of the event [10, 11]. The discriminating power of these variables steams from the fact that the most severe background, coming from the $q\overline{q}$ creation in e^+e^- collisions, is frequently accompanied by a photon radiated off the initial state which results in a smaller effective CMS energy. Jets from $q\overline{q}(\gamma)$ events are also expected to be distributed less uniformly than jets from the W-pair decays. A similar set of variables was used to describe the shape of mixed W^+W^--decays: the probability for the kinematically constrained fit, the effective CMS energy, the total multiplicity, the aplanarity of the event, the transverse missing momentum, and the number of reconstructed jets and their angular distribution. In addition, for mixed decays with electrons or muons the momentum spectrum of the lepton candidates was also also exploited as well as the distribution of the events with respect to the angle between the lepton and the direction of the missing momentum, the muon and electron identification criteria in the DELPHI detector, and the isolation of the lepton candidates from the rest of the event. The latter was defined by the energy, deposited inside a 10° cone around the lepton direction. The isolation of tau-jet candidates was, on the other hand, defined in terms of the energy of

charged particles inside a 30° cone around the τ-candidate. Tau jet candidates were also tried to be distinguished from the rest of hadronic jets and missassociated tracks by the number of the tracks in the jet and, as in the case of electrons and muons, by the angle that they formed with the missing momentum direction.

Relying on the corresponding simulated distributions, one can calculate a probability that a measured event with a given value of a particular variable originates from a W-pair decay. By multiplying probabilities from all listed quantities for each of the three classes single discriminating variables P_{4q}, $P_{2qe(\mu)\nu}$ and $P_{2q\tau\nu}$ were obtained. To avoid multiple counting, every event was put in the class with the largest value of the discriminating variable. Due to the small number of events the two classes of mixed decay candidates were then merged into one common class. Figure 2 shows the measured distributions for fully hadronic and mixed decay events according to the separating variables, as well as the expected distributions from corresponding simulated W^+W^--decays and from the background. For further analysis only events on the right of the arrows were taken into account in order to maximize the product of the selection efficiency and the purity of the selected samples.

After the selection, the flavour-tagging of the jets was applied. The tagging relies on the information from the DELPHI vertex and tracking detectors and on the charged particle identification with the RICH counters. In order to separate jets, originating from primary quarks with different flavours, the following discriminating properties were used:

- c- and s-jets can be tagged by the high momentum charged kaons, detected in the system of DELPHI RICH counters. These kaons are very likely to contain a primary s-quark or an s-quark from a $c \to s$ decay. Figure 3.a shows the expected spectra for the leading particles identified as charged kaons in jets with c-, s-, u- and d- flavour, respectively. Using the same arguments, if a fast particle in a hadronic jet is an identified pion it is an indication for a u- or d-jet (see Fig. 3.b for illustration). In each jet, the momentum dependent probability for a particular jet flavour was calculated by considering only the fastest identified particle in the jet. In addition, such a particle was required to be among the leading three particles in the jet. To distinguish between quarks and antiquarks of the same flavour the charge of identified particles is also used.

  As a minor contribution to the flavour separation, the momentum distribution of identified muons, neutral kaons and Λ-baryons was also used. Muons are a signature for semileptonic decay of charm hadrons, while reconstructed K^0_S's and Λ's serve as an indication for a primary s-quark.

- c-jets can also be separated from the s-, u- and d-jets by the lifetime tag that is based upon the impact parameter distribution of particles, ascribed to a particular jet [5, 13]. From this distribution one can build a probability that all particles in a jet originate from the primary vertex. This probability is, due to the finite lifetime and the larger mass of the c-quark, smaller for charm than for light-quark jets (see Fig. 4).

In the same way as in the event selection procedure, the described flavour signatures were combined into probabilities $P(q)$ for each jet to originate from a c-, s-, u- or d-quark. The impact of the combinatorial background was reduced by exploiting the correlation between the direction of a jet and the flavour of its primary quark. Namely, W^+'s produced in e^+e^- collisions are partly polarized along their momenta and W^-'s in the opposite direction [14]. Therefore, because of the $V-A$ structure of the W-decays, down-like quarks and anti-quarks, i.e. s,d,$\overline{s}$ and $\overline{d}$, will fly mainly along the momentum of the parent W (Fig. 5.a). The twofold

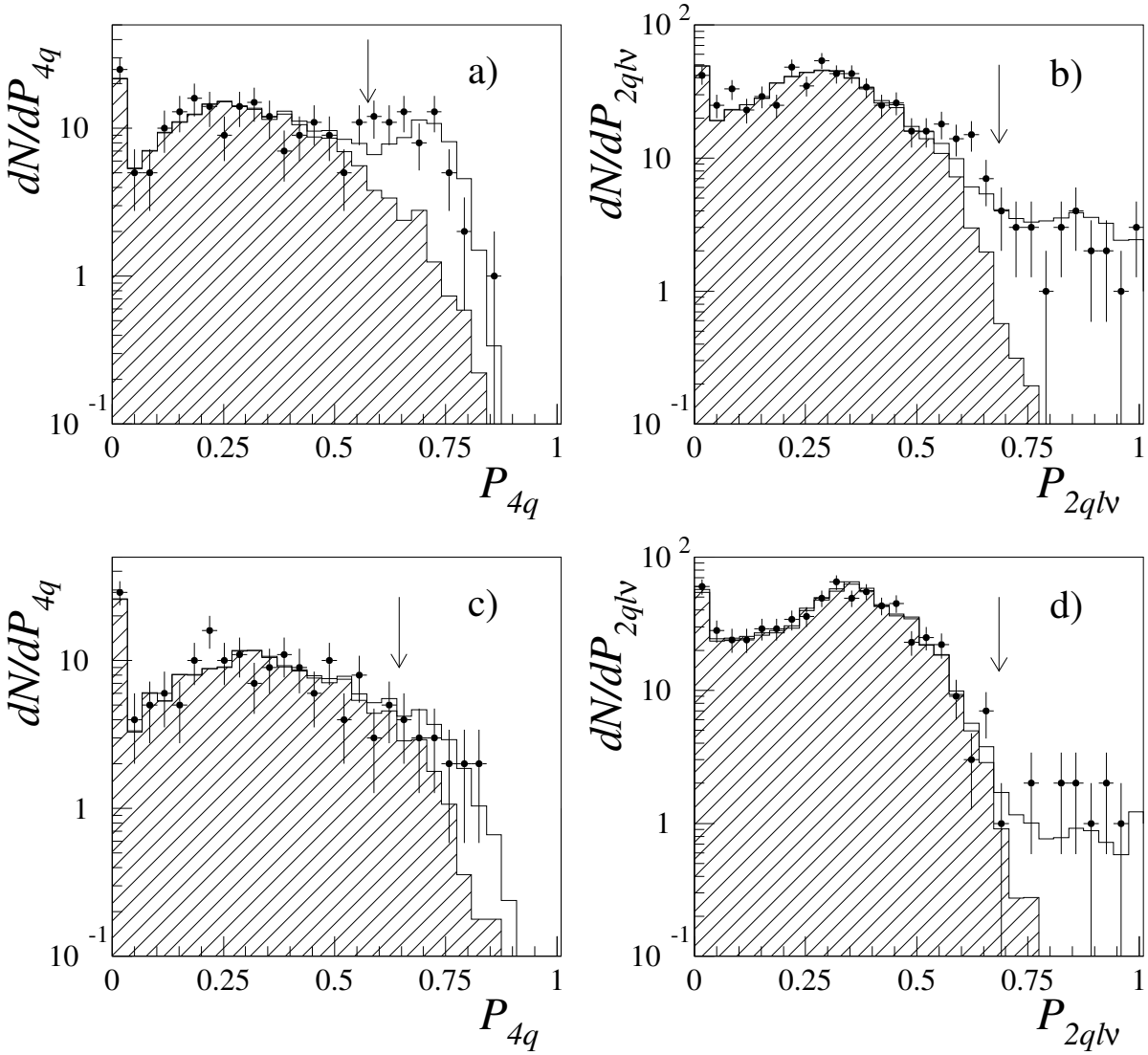

Figure 2: Distributions of events in selected classes with respect to the discriminating variables for the two classes: fully hadronic candidates (a) and c)) and candidates for mixed decays (b) and d)). The upper row shows distributions for 172 GeV energy and the lower row for 161 GeV. Measured spectra are displayed as dots with error bars, expected signals as open histograms and background as hatched histograms. The background is a sum of contributions from $q\overline{q}(\gamma)$, $We\nu$, ZZ, Ze^+e^-, $e^+e^-\gamma$ and two-photon production in e^+e^- interactions.

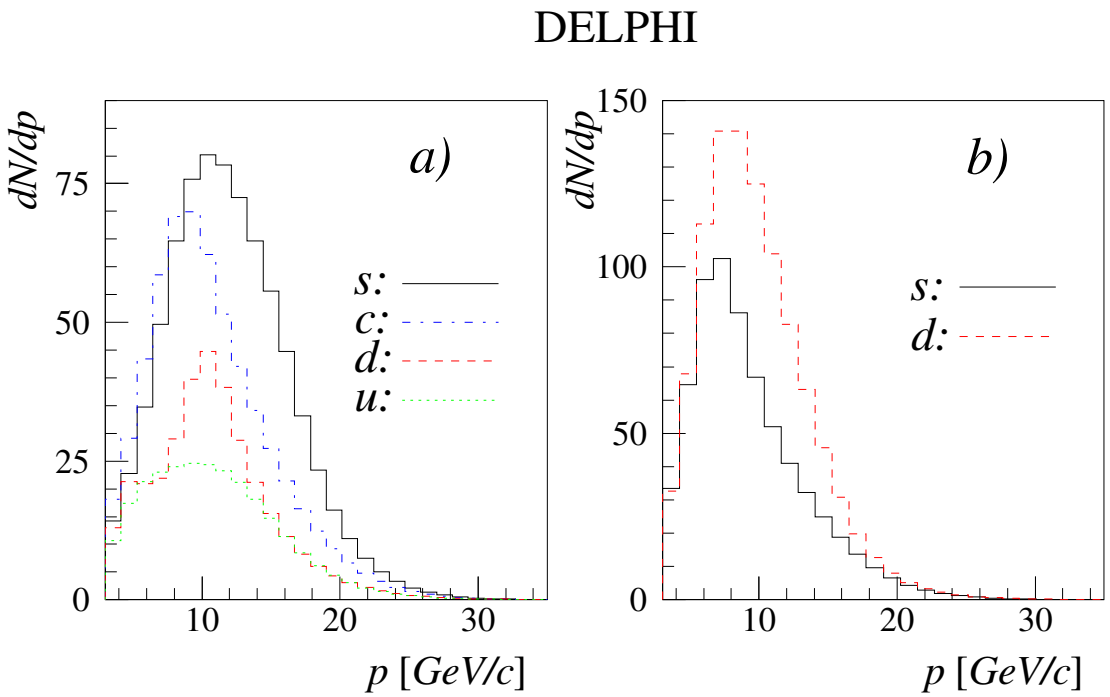

Figure 3: a) Momentum spectra of identified charged kaons in simulated c-, s-, u- and d- jets when the kaon is the leading particle in the jet. b) Momentum spectra of leading particles, identified as pions in d- and s-jets, respectively. The number of entries in Figs. 3 and 4 corresponds to approximately 15000 generated W^+W^- events.

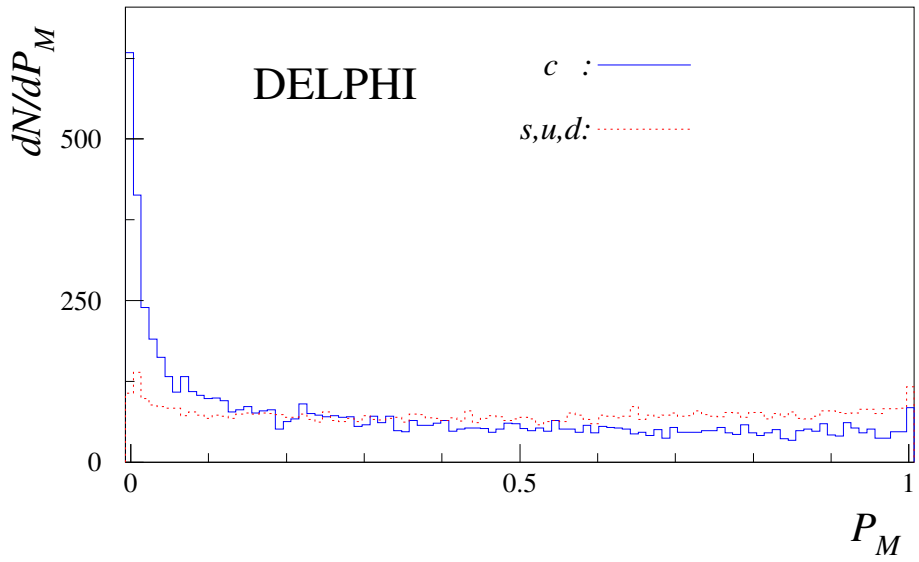

Figure 4: Simulated distributions of the probabilities P_M that all charged particles in a jet come from the main vertex, for c-jets (full histogram) and for s-, u- or d-jets (dotted histogram).

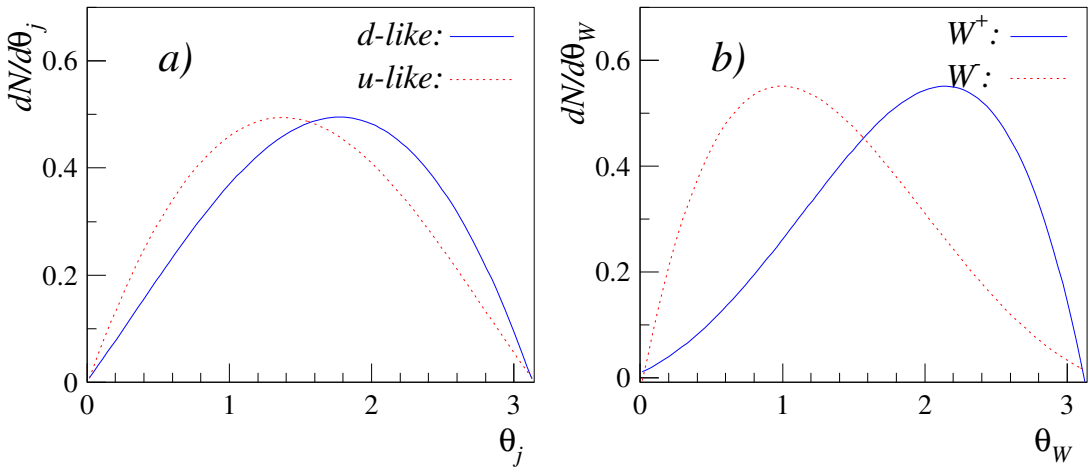

Figure 5: a) Simulated distribution of the angle between the momenta of the W's and the of corresponding jets from down-like (solid line) or up-like (dotted line) quarks from the W's decays at a centre-of-mass energy of 172 GeV. b) Angular distributions of W^+'s (solid line) and of W^-'s (dotted line) with respect to the direction of the positron beam.

ambiguity whether the down-like quark is really a quark (d or s) or an antiquark ($\overline{d}$ or $\overline{s}$) can further be resolved by determining the charge of the parent W. In four-jet events one can determine the sign of the W-charge by making use of the strong correlation between the direction of the W's and their charge [14, 15]. Namely, momenta of positively charged gauge bosons point mainly into the hemisphere, determined by the direction of the positron beam (Fig. 5.b). In $q\overline{q}l\overline{\nu}$ decays, the charge of the W's was determined by the charge of lepton candidates from leptonic W-decays. The correlations between the jet direction and the flavour of the primary quark were then incorporated into the probabilities $P(q)$. Note, however, that the polarization of the $W^{\pm}$'s (Fig. 5.a), and thus also the background rejection power, substantially increase with the increasing e^+e^- CMS energy, attainable in the coming years of LEP-2.

When combining the flavours of the two jets from hadronic $W^{\pm}$-decays, for different combinations were considered:

$$c\overline{s},\ \overline{c}s,\ u\overline{d},\ \text{and}\ \overline{u}d\ .$$

Decays into $b\overline{c}$, $u\overline{s}$ and $c\overline{d}$ pairs are strongly Cabibbo-suppressed: they were considered as a minor contribution to the $u\overline{d}$ and $\overline{u}d$ combinations (see below).

As the final separator, the probability P_{cs} was constructed that two jets come from the decay $W^+ \to c\overline{s}$:

$$P_{cs} = \frac{P_1(c)P_2(\overline{s}) + P_2(c)P_1(\overline{s}) + P_1(\overline{c})P_2(s) + P_2(\overline{c})P_1(s)}{K_{\rm nor}}\ ,$$

where $K_{\rm nor}$ is a normalization constant:

$$\begin{aligned} K_{\rm nor} &= P_1(c)P_2(\overline{s}) + P_2(c)P_1(\overline{s}) + P_1(\overline{c})P_2(s) + P_2(\overline{c})P_1(s) \\ &+ P_1(u)P_2(\overline{d}) + P_2(u)P_1(\overline{d}) + P_1(\overline{u})P_2(d) + P_2(\overline{u})P_1(d)\ . \end{aligned}$$

Indices 1 and 2 refer to the first and to the second jet in a di-jet combination, respectively. Figure 6 shows the P_{cs} distributions, expected for $c\overline{s}$ and for $u\overline{d}$ di-jets from $W^{\pm}$-decays.

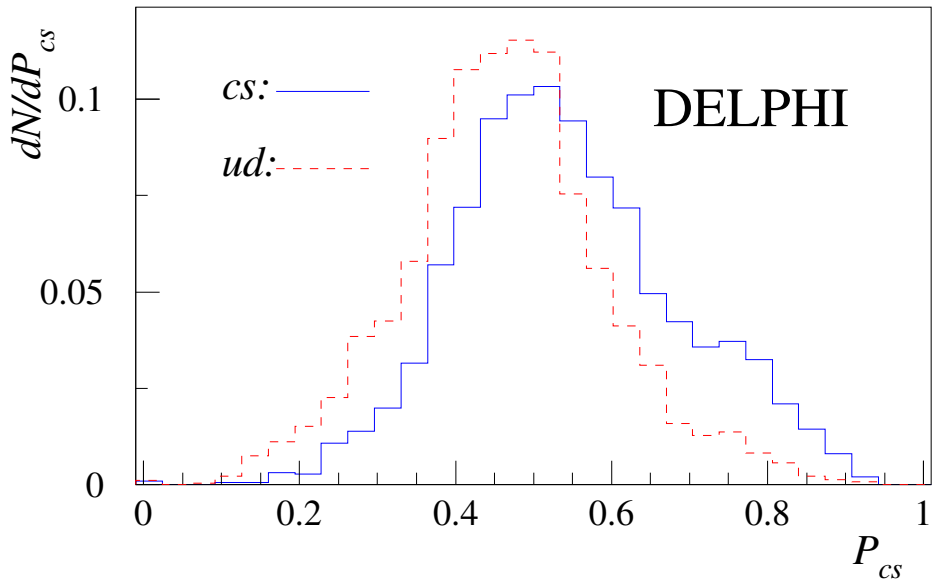

Figure 6: P_{cs} distributions for simulated $c\overline{s}$-jets (full histogram) and $u\overline{d}$-jets (dashed histogram).

5 Determination of the $|V_{cs}|$ by tagging the flavour of the jets

The value of the $|V_{cs}|$ was extracted from the data by fitting the expected P_{cs} distributions to the spectra of the selected di-jet combinations by using the maximum-likelihood method. The likelihood function

$$L = Mn(N; N_1, N_2, ..., N_i, ...; p_1, p_2, ..., p_i, ...)$$

was constructed as a multinomial probability [16] to observe N_1 out of N measured di-jets in the first bin of the P_{cs} distribution, N_2 in the second bin, etc. The probability p_i that a di-jet, randomly picked up from the selected sample of WW-candidates, would fall into the i-th bin, depends on the value of the $|V_{cs}|$ and was determined by the simulated signal and background samples.

The P_{cs} distributions, extracted from the selected $jjjj$ and $jjl\overline{\nu}$ candidates, were fitted simultaneously, with the migrations between the two channels properly taken into account. The fit was performed by the MINUIT program package [17].

Figure 7 shows the measured P_{cs} spectra together with accommodated expected distributions, while fractions of particular contributions to the overall P_{cs} spectrum are displayed in Figure 8. The fitted value of the $|V_{cs}|$ is

$$|V_{cs}| = 0.87 \begin{array}{c}+0.26\\-0.22\end{array} \text{ (stat) } \pm 0.11 \text{ (syst)}.$$

The list of the contributions to the overall systematic error is given in the next section.

The value of the $|V_{cs}|$, extracted by the flavour tagging of jets, can also be converted into the ratio of hadronic W^+ decays into the $c\overline{s}$ quarks:

$$r^{(cs)} = \frac{\Gamma(W^+ \to c\overline{s})}{\Gamma(W^+ \to \text{hadrons})} = 0.42 \begin{array}{c}+0.14\\-0.12\end{array} \text{ (stat) } \pm 0.06 \text{ (syst)} .$$

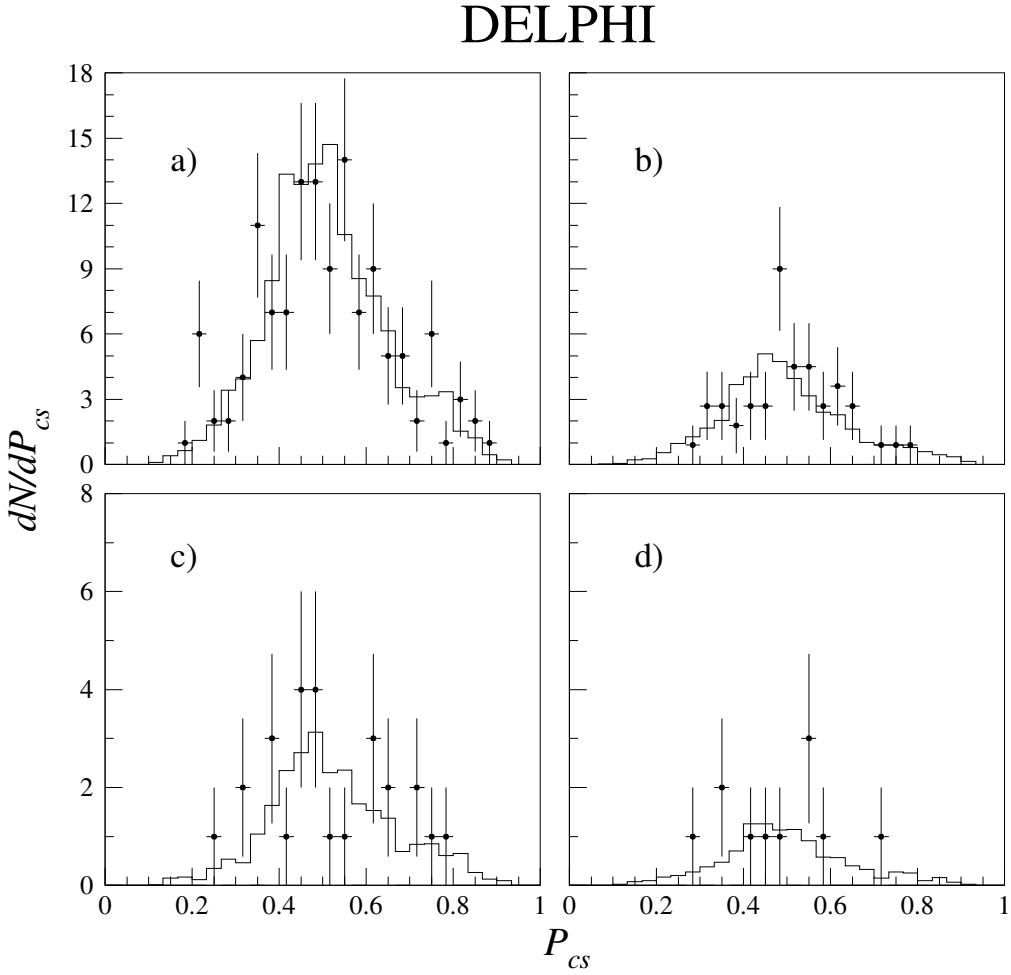

Figure 7: Measured P_{cs} spectra (points with error bars) together with the best fit simulated predictions (histograms) for $jjjj$ decays (a) and c)) and for $jjl\overline{\nu}$ events (b) and d)). Figures a) and b) correspond to the data, taken at 172 GeV centre-of-mass energy, while the data, shown in the lower row, were collected at 161 GeV.

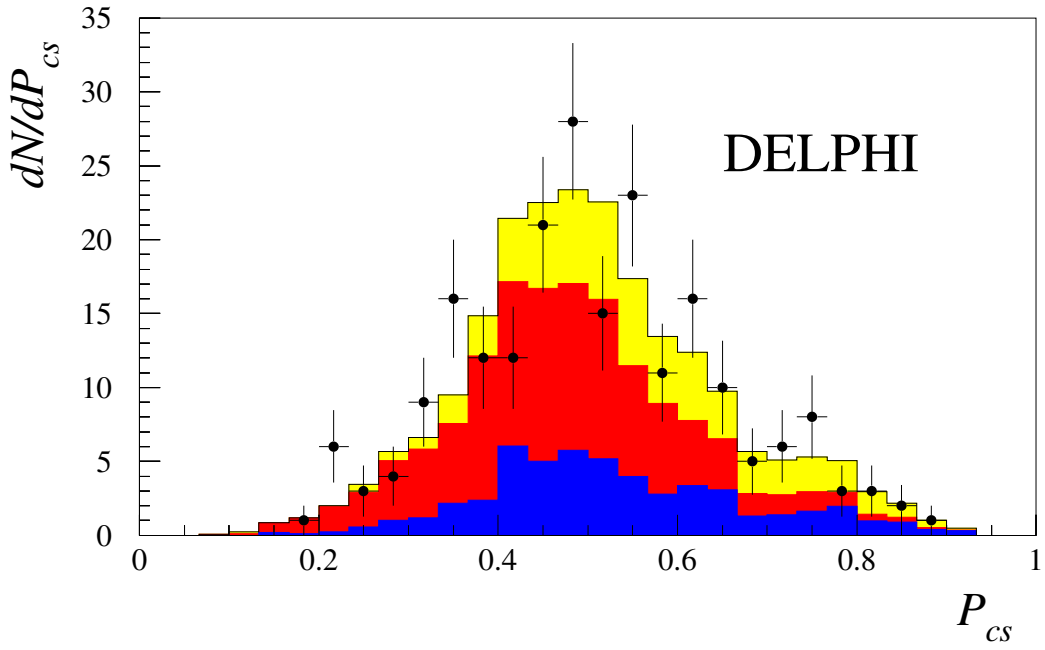

Figure 8: The sum of the $jjjj$ and the $jjl\overline{\nu}$ P_{cs} spectra. Measured distribution is shown by the points with error bars and the best fit with the histogram. The shaded areas show fractions of particular contributions: $W^+ \to c\overline{s}$ (lightest shading), $W^+ \to u\overline{d}$ together with the Cabibbo-suppressed decays, and the background (darkest shading).

6 Systematic uncertainties on the $|V_{cs}|$

The systematic uncertainties on the $|V_{cs}|$, extracted from the measured hadronic branching ratio of the $W^{\pm}$ [9], are dominated by the uncertainties on the background normalization for the fully hadronic W^+W^--decays, and by the error on the efficiency calculation (see Table 1). Apart from the Feynman diagrams, involving W-pairs (the so-called "CC03 diagrams" [15], containing s-channel γ and Z exchange and t-channel ν exchange), there are also other electroweak diagrams involving either zero, one or two massive vector bosons, which can lead to the same final state fermions. The effects of the interference between the CC03 diagrams and the additional diagrams were estimated by using the four-fermion generator EXCALIBUR [18], and have been treated as additional correction factors to the absolute normalization [9, 10] of the expected signal. The possible uncertainties on these values were added to the overall systematic error of the measurement (Table 1). In addition, the contributions due to the uncertainties on the values of the $|V_{cd}|$ and on the strong coupling constant $\alpha_S(M_{W^{\pm}})$ [3] were also considered. They were found to be small (Table 1), while impact of errors on other parameters of the Standard Model is negligible.

The systematic error on the $|V_{cs}|$, measured by tagging the flavour of hadronic jets from the W-decays, is determined mainly by the precision of tuning the DELPHI tracking detectors and fragmentation models in the generators of simulated events. The systematic uncertainty on the lifetime tag was estimated by using the Z^0 hadronic decays, collected during the short runs at the Z^0 pole during the 1996. Samples with different fractions of $b\overline{b}$, $c\overline{c}$ and light-quark decays were selected by cutting at different values of the probability P_M that all charged tracks in one hemisphere come from the primary vertex (see Section 5). Then measured and simulated P_M distributions in the other hemispheres were compared. Although the simulated and the

Table 1: The list of contributions to the systematic uncertainties on the measurement of the $|V_{cs}|$ for the two methods and for the combined result. Note that for the first method the error due to the finite Monte Carlo (MC) sample is included in the error coming from the efficiency calculation.

	Contribution to the systematic error on $\|V_{cs}\|$		
Source of uncertainty	From BR($W^{\pm} \to q\overline{q}$)	With flavour tag	Combined
Efficiency calculation	± 0.027	-	± 0.019
Background normalization	± 0.028	± 0.003	± 0.021
"CC03"-correction factors	± 0.015	< 0.001	± 0.010
$\|V_{cd}\|$	± 0.004	< 0.001	± 0.003
α_S	± 0.001	< 0.001	± 0.001
Lifetime tag	-	± 0.090	± 0.031
$K^{\pm}$,$\pi^{\pm}$ spectra	-	± 0.040	± 0.012
MC statistics	-	± 0.040	± 0.012
Combined	± 0.042	± 0.106	± 0.046

measured distributions were compatible within the errors, the small differences were interpreted as a possible disagreement between the simulation and the data. the P_M distributions, used in calculation of the $P(q)$ for u-, d-, s- and c-jets, were varied according to these differences. The resulting variation of $|V_{cs}|$ was found to be ± 0.09. The tuning of the parameters of the fragmentation model, used in the process of event simulation, was checked with samples of particles collected at the Z^0-pole and during high-energy runs in 1996, as well as with the large number of measured Z^0 decays detected during the operation of LEP-1. In a similar way as for the estimation of the lifetime tag systematic uncertainties, $c-$, $s-$, or $u/d-$enhanced samples were selected by cutting at different values of the P_M and by requiring identified fast kaons or pions in one hemisphere. The momentum spectra of fast kaons and pions in the other hemisphere were then compared to the appropriate simulated distributions. The small observed disagreement between the measured and simulated spectra was taken and the simulated spectra, used for the construction of the expected P_{cs} distributions, were modified bin-by-bin. In this way a systematic uncertainty of ± 0.04 on the $|V_{cs}|$ was determined.

7 Conclusion

To conclude, the sample of the W-pairs, collected by the DELPHI detector during the first year of the LEP high energy run, was exploited to measure the value of the $|V_{cs}|$ element of the CKM matrix. The value, extracted from the measured hadronic branching ratio of the W-boson, is

$$|V_{cs}| = 0.90 \ \pm 0.17\,(\mathrm{stat}) \ \pm 0.04\,(\mathrm{syst})\ ,$$

while tagging the flavour of jets from W-decays gives

$$|V_{cs}| = 0.87 \begin{array}{c}+0.26\\-0.22\end{array} \,(\mathrm{stat}) \;\pm 0.11\,(\mathrm{syst})\;.$$

The precision of the two values combined,

$$|V_{cs}| = 0.89 \begin{array}{c}+0.14\\-0.13\end{array} \,(\mathrm{stat}) \;\pm 0.05\,(\mathrm{syst})\;,$$

already surpasses the precision of the combination of all previous measurements [19, 20, 21, 22]. Moreover, unlike the accuracy of the previous measurements, limited by the uncertainties from the theoretical input, the uncertainty on this result is dominated by the statistical error. Until the end of LEP-2 it can be therefore expected that the precision will be substantially improved.

Acknowledgement

It is a pleasure to thank our technical collaborators and the funding agencies for their support in building and operating the DELPHI detector. At the same time, we are also greatly indebted to the members of the CERN-SL Division for the excellent performance of the LEP collider.

References

[1] N.Cabibbo, Phys.Rev.Lett. **10** (1963) 531.

[2] M.Kobayashi,T.Maskawa, Progr.Theor.Phys. **49** (1973) 652.

[3] Particle Data Group, Review of Particle Physics, Phys.Rev. **D54** (1996) 1.

[4] DELPHI Collaboration, P.Aarnio et al, Nucl.Instr.Meth. **A303** (1991) 233.

[5] DELPHI Collaboration, P.Abreu et al., Nucl.Instr.Meth. **A378**, (1996) 57.

[6] T.Sjöstrand, *PYTHIA 5.7 / JETSET 7.4*, CERN-TH.7112/93 (1993).

[7] DELPHI Collaboration, P.Abreu et al., Z. Phys. **C73** (1996) 11.

[8] A.Ballestrero et al., *Determination of the Mass of the W Boson*, Physics at LEP2, eds. G.Altarelli, T.Sjöstrand and F.Zwirner, CERN 96-01 (1996) Vol. 1, p. 141.

[9] DELPHI Collaboration, P.Buschmann et al., *Measurement of the W-pair cross-section and of the W mass in e^+e^- interactions at 172 GeV*, DELPHI note 97-108 CONF 90; Paper #347 submitted to the HEP'97 Conference, Jerusalem, August 19-26.

[10] DELPHI Collaboration, P.Abreu et al., *Measurement and interpretation of the W-pair cross-section in e^+e^- interactions*, CERN-PPE 97-09, submitted to Phys. Lett. B.

[11] P.Abreu, D.Fassouliotis, A.Grefrath, R.P.Henriques, L.Vitale, *SPRIME, A Package for Estimating the Effective $\sqrt{s'}$ Centre of Mass Energy in $q\overline{q}(\gamma)$ Events*, Delphi Note 96-124 PHYS 632.

[12] N.Kjaer, R.Möller, *Reconstruction of Invariant Masses in Multijet Events*, Delphi Note 91-17 PHYS 88.

[13] G.Borisov, *Lifetime Tag of Events $Z^0 \to b\bar{b}$ with the DELPHI Detector*, Delphi Note 94-125 PROG 208.

[14] Z.Ajaltouni et al., *Triple Gauge Boson Couplings*, Physics at LEP2, eds. G.Altarelli, T.Sjöstrand and F.Zwirner, CERN 96-01 (1996) Vol. 1, p. 525.

[15] W.Beenakker, F.A.Berends et al., *WW cross section and distributions*, Physics at LEP2, eds. G.Altarelli, T.Sjöstrand and F.Zwirner, CERN 96-01 (1996) Vol. 1, p. 79.

[16] W.T.Eadie, D.Drijard, F.E.James, M.Roos, B.Sadoulet, *Statistical Methods in Experimental Physics*, North-Holland (1971).

[17] Application Software Group, CN division CERN, *MINUIT Function Minimisation and Error Analysis*, CERN Program Library Long Writeup D506.

[18] F.A.Berends, R.Kleiss, R.Pittau,et al., *EXCALIBUR*, Physics at LEP2, eds. G.Altarelli, T.Sjöstrand and F.Zwirner, CERN 96-01 (1996) Vol. 2, p. 23.

[19] H.Abramowicz et al., Z.Phys. **C15** (1982) 19.

[20] CLEO Collaboration, A.Bean et al., Phys.Lett. **B317** (1993) 647.

[21] Mark III Collaboration, Z.Bai et al., Phys.Rev.Lett. **66** (1991) 1011.
Mark III Collaboration, J.Adler et al., Phys.Rev.Lett. **62** (1989) 1821.

[22] E691 Collaboration, J.R.Raab et al., Phys.Rev. **D37** (1988) 2391.